Environmental Science & Technology

Get it@ULg

Subscriber access provided by Université de Liège

Article

Mercury stable isotopes discriminate different populations of European seabass and trace potential Hg sources around Europe

Alice A.E. Cransveld, David Amouroux, Emmanuel Tessier, Emmanuil Koutrakis, Ayaka Amaha Ozturk, Nicola Bettoso, Cláudia L Mieiro, Sylvain Berail, Julien P. G. Barre, Nicolas Sturaro, Joseph G. Schnitzler, and Krishna Das

Environ. Sci. Technol., **Just Accepted Manuscript** • DOI: 10.1021/acs.est.7b01307 • Publication Date (Web): 25 Sep 2017

Downloaded from http://pubs.acs.org on September 26, 2017

Just Accepted

"Just Accepted" manuscripts have been peer-reviewed and accepted for publication. They are posted online prior to technical editing, formatting for publication and author proofing. The American Chemical Society provides "Just Accepted" as a free service to the research community to expedite the dissemination of scientific material as soon as possible after acceptance. "Just Accepted" manuscripts appear in full in PDF format accompanied by an HTML abstract. "Just Accepted" manuscripts have been fully peer reviewed, but should not be considered the official version of record. They are accessible to all readers and citable by the Digital Object Identifier (DOI®). "Just Accepted" is an optional service offered to authors. Therefore, the "Just Accepted" Web site may not include all articles that will be published in the journal. After a manuscript is technically edited and formatted, it will be removed from the "Just Accepted" Web site and published as an ASAP article. Note that technical editing may introduce minor changes to the manuscript text and/or graphics which could affect content, and all legal disclaimers and ethical guidelines that apply to the journal pertain. ACS cannot be held responsible for errors or consequences arising from the use of information contained in these "Just Accepted" manuscripts.

ACS Publications

Environmental Science & Technology is published by the American Chemical Society. 1155 Sixteenth Street N.W., Washington, DC 20036

Published by American Chemical Society. Copyright © American Chemical Society. However, no copyright claim is made to original U.S. Government works, or works produced by employees of any Commonwealth realm Crown government in the course of their duties.

Mercury stable isotopes discriminate different populations of European seabass and trace potential Hg sources around Europe

Alice Cransveld *[,a], David Amouroux[b], Emmanuel Tessier[b], Emmanuil Koutrakis[c], Ayaka A Ozturk[d], Nicola Bettoso[e], Cláudia L. Mieiro[f], Sylvain Bérail[b], Julien P. G. Barre[b], Nicolas Sturaro[a], Joseph Schnitzler[a,g], Krishna Das*[,a]

a. Laboratory for Oceanology - MARE, University of Liège, 15 Allée du 6 Août, 4000 Liège, Belgium

b. CNRS/ UNIV PAU & PAYS ADOUR, Institut des Sciences Analytiques et de Physico-Chimie pour l'Environnement et les Materiaux, UMR5254, 64000, PAU, France

c. Fisheries Research Institute, Hellenic Agricultural Organisation, 640 07 Nea Peramos, Kavala, Greece

d. Faculty of Fisheries, Istanbul University, Turkey

e. Agenzia Regionale per la Protezione dell'Ambiente del Friuli Venezia Giulia (ARPA FVG), via A. La Marmora 13, 34139 Trieste, Italy

f. CESAM and Departamento de Biologia, Universidade de Aveiro, Campus Universitário de Santiago, 3810-193 Aveiro, Portugal

g. Institute for Terrestrial and Aquatic Wildlife Research, University of Veterinary Medicine Hannover, Foundation, 25761 Büsum, Schleswig-Holstein, Germany.

* Address correspondence to either author. Email: alice.cransveld@gmail.com; krishna.das@ulg.ac.be . Phone: +32 (0)4 366 33 21/Fax : +32 (0)4 366 5147

Abstract

Our study reports the first data on mercury (Hg) isotope composition in marine European fish, for seven distinct populations of the European seabass, *Dicentrarchus labrax*. The use of δ^{202}Hg and Δ^{199}Hg values in SIBER enabled us to estimate Hg isotopic niches, successfully discriminating several populations. Recursive-partitioning analyses demonstrated the relevance of Hg stable isotopes as discriminating tools. Hg isotopic values also provided insight on Hg contamination sources for biota in coastal environment. The overall narrow range of δ^{202}Hg around Europe was suggested to be related to a global atmospheric contamination while δ^{202}Hg at some sites was linked either to background contamination, or with local contamination sources. Δ^{199}Hg was related to Hg levels of fish but we also suggest a relation with ecological conditions. Throughout this study, results from the Black Sea population stood out, displaying a Hg cycling similar to fresh water lakes. Our findings bring out the possibility to use Hg isotopes in order to discriminate distinct populations, to explore the Hg cycle on a large scale (Europe) and to distinguish sites contaminated by global versus local Hg source. The interest of using Hg sable isotopes to investigate the whole European Hg cycle is clearly highlighted.

TOC Art:

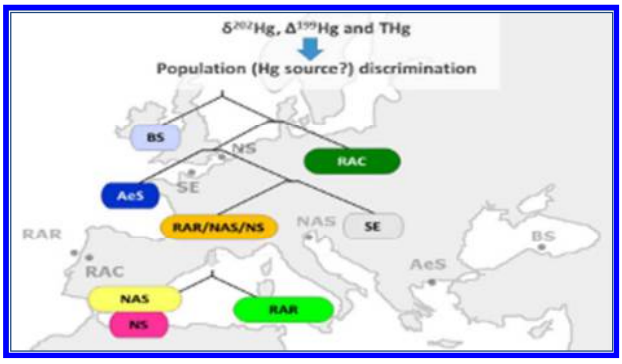

1. Introduction

Mercury (Hg) is a persistent toxic element that has the capacity to biomagnify and bioaccumulate, particularly when present under its organic form, methylmercury (MeHg), which poses serious health risks[1]. Although it is naturally present in ecosystems, human activities have increased the amount of actively cycling Hg, by an estimated factor of 3 to 5 since industrialization[2]. Emissions are currently strictly regulated by numerous institutions: the OSPAR commission pointed out Hg as a priority pollutant[3], the United Nations Environment Programme (UNEP) recently launched a legally binding global mercury convention in order to minimize further anthropogenic Hg release into the environment[4]. Despite regulations, levels still found in marine predators (teleosts and marine mammals) are still above environmental quality standards [3,5–9], illustrating the many uncertainties that still exist in the comprehension of Hg's biochemistry at both regional and global scales[10].

Anthropogenic mercury sources to the environment are mainly fossil fuel combustion, mining, and industrial activities (*e.g.* chlor-alkali industry). Hg can be emitted in gaseous elemental form (Hg^0), which has a long residence time in the atmosphere (0.5-1.5 years)[11], allowing it to travel long distances and have an impact at a global scale. Hg releases can also occur in solid or liquid form, with wastewater for instance, impacting primarily the vicinity of mining and industrial sites (regional scale)[12].

Methylation of inorganic Hg (IHg) is generated by microbial activity and can take place both in coastal sediments and in open ocean water column[13,14]. External MeHg sources such as fluvial and tidal waters are also playing a role in marine food web contamination [15]. MeHg can also be demethylated by sunlight induced degradation pathways[14,16]. Microbial activity and both dark and photochemical abiotic reactions ultimately control the chemical speciation and subsequent bioavailability of Hg[13,14].

Recently, the study of the seven Hg stable isotopes have enhanced the understanding of the sources of Hg and of the competing processes that produce and degrade MeHg in natural environment[13,15,16]. Mercury stable isotopes display both mass dependent fractionation (MDF, reported as δ^{202}Hg) and mass independent fractionation (MIF, reported as Δ^{199}Hg and Δ^{201}Hg)[17]. MDF concerns all Hg isotopes and has been documented in all biotic and abiotic chemical reactions that have been investigated, such as biotic methylation[18], demethylation[19], passive diffusion and photochemical reactions[16].

While some studies show that fish MeHg is derived from the Hg present in the local sediment, others have indicated that MeHg from different or additional sources might be accumulated by biota, especially in coastal environment[15,20]. Interestingly, such external MeHg sources could display a distinct δ^{202}Hg. In the past decade, δ^{202}Hg and Δ^{199}Hg values have successfully been exploited in order to trace contamination sources in ecosystems[12,21–25], but also to investigate exposure pathways, bioaccumulation and trophic transfer of MeHg in marine food webs [15,26–28].

In this study, we use Hg stable isotopes combined with mercury concentration and speciation, as well as carbon (C) and nitrogen (N) stable isotopes (used to estimate trophic level) to investigate the sources and exposure pathways of Hg of a marine predator across Europe. We sampled the European seabass, *Dicentrarchus labrax*, in 7 different sites and analyzed muscle tissue. The objectives of this study were to (1) determine and compare the Hg stable isotopic niche of marine predators from different geographical areas in Europe (2) give insights on MeHg cycling and pathways (3) potentially distinguish between distinct Hg sources (*e.g.* local vs global). To fulfill our objectives, we started by comparing Hg levels between sites and by investigating the possible causes of observed variability.

2. Materials and methods

96

97 **Species description**

98 Our model species is the European seabass, *Dicentrarchus labrax*. It is a largely distributed, abundant
99 species. As a second order marine predator when fully-grown, it accumulates significant
100 concentrations of pollutants[29,30]. Moreover, juveniles are sedentary and very commonly found in
101 estuaries[31] which are particularly affected by pollution. Here juveniles whose length ranged from 16
102 to 35 cm were sampled, so they would reflect the environment where they were caught and still
103 potentially display high levels of contamination.

104

105 **Site description**

106 Fish were collected between 2012 and 2014 from 7 coastal sites throughout Europe (Figure S-1)
107 located in: the North Sea (NS), the Northern Aegean Sea (AeS), the Seine Estuary (SE), the Northern
108 Adriatic Sea (NAS), the Turkish coast of the Black Sea (BS), and two different sites at the Ria de Aveiro
109 in Portugal (the "reference" site and the "contaminated" site - RAR and RAC). The distribution of
110 sampling sites spanned across different latitudes and water quality, including areas influenced by
111 riverine effluents from mining and chlor-alkali industries[21,32]. (Description of sites in SI.)

112

113 **Sample collection**

114 After sampling, fish were kept in freezers at -20°C or less (-80°C). Prior to dissection, fish were
115 thawed, measured (snout to fork), and weighed. Muscles were sampled for each specimen. Muscle
116 was chosen because it is an abundant tissue, known to accumulate high Hg concentrations, and is
117 closely related with risks of human contamination[33]. We also took scales from under the left pectoral
118 fin, and investigated stomach content (Table S-1). Muscle samples were freeze-dried, ground into a
119 homogenous powder, then stored in the dark before use. Water content of muscle was determined.
120 Age determination was performed by observing the scales under a binocular and counting the
121 number of annual growth marks, called annuli as described previously[34].

Analyses

Sample analysis follows previously described protocols and are presented here briefly. (Details in the SI.)

Carbon and Nitrogen isotope composition were measured by an isotope ratio mass spectrometer as detailed elsewhere[35]. In order to allow inter-population comparison, we also calculated each individual's trophic level (TL) after Post[36]. Total Hg (THg) concentrations were determined on a Milestone Direct Mercury Analyzer 80[37]. T-Hg concentration is expressed $ng.g^{-1}$ dry weight (DW). MeHg and IHg concentrations were determined by isotope dilution-gas chromatography-inductively coupled plasma-mass spectrometer (ID-GC-ICP-MS) following microwave-assisted extraction and aqueous phase derivatization, as detailed elsewhere [38]. Reference material included BCR CRM-464 (tuna fish muscle, from Adriatic Sea, certified for MeHg and THg concentration), and DOLT-4 (dogfish liver) (Table S-3).

Mercury isotopic composition analysis was performed using cold vapor generation (CVG) with multi-collector-inductively coupled plasma-mass spectrometer (MC-ICP-MS, Nu Instruments). A desolvation nebulisation system from Nu Instrument was used to introduce NIST-SRM-997 thallium for instrumental mass-bias correction using the exponential fractionation law. Reference material UM-Almaden and BCRCRM-464 were used as secondary standards (Table S-4). We used a standard-sample bracketing system to calculate δ values (in ‰) relative to the reference standard NIST SRM 3133 mercury spectrometric solution. Isotope ^{198}Hg was used as the reference for ratio determination of all other Hg isotopes, using the following equations:

$$\delta^{xxx}\mathrm{Hg} = \left[\frac{(^{xxx}\mathrm{Hg}/^{198}\mathrm{Hg})_{\mathrm{sample}}}{(^{xxx}\mathrm{Hg}/^{198}\mathrm{Hg})_{\mathrm{NIST\ 3133}}} - 1)\right] \times 1000 \qquad (2)$$

$$\Delta^{199}\mathrm{Hg} = \delta^{199}\mathrm{Hg}_{\mathrm{observed}} - \delta^{199}\mathrm{Hg}_{\mathrm{predicted}} = \delta^{199}\mathrm{Hg}_{\mathrm{observed}} - (\delta^{202}\mathrm{Hg} \times 0.252) \quad (3)$$

$$\Delta^{201}\mathrm{Hg} = \delta^{201}\mathrm{Hg}_{\mathrm{observed}} - \delta^{201}\mathrm{Hg}_{\mathrm{predicted}} = \delta^{201}\mathrm{Hg}_{\mathrm{observed}} - (\delta^{202}\mathrm{Hg} \times 0.752) \quad (4)$$

Statistical analyses

The SIBER (Stable Isotope Bayesian Ellipse in R) package from R was used to estimate the isotopic niche (trophic niche and Hg niche) of each population[39]. SIBER was used to generate bivariate standard ellipses that represent core isotopic niches of the different populations of seabass. Areas of the ellipses associated to each site (Standard Ellipse Area, SEA) were computed using Bayesian modeling (10^6 iterations). Applying SIBER to Hg stable isotopes (δ^{202}Hg and Δ^{199}Hg) constitutes the first attempt to define Hg isotopic niche through SIBER.

To identify whether Hg variables (THg, MeHg, %MeHg, δ^{202}Hg and Δ^{199}Hg) effectively enables the discrimination of different populations of fish, we developed decision trees using recursive partitioning (Rpart package [version 4.1-10][40] incorporated in R package [version 3.2.3][41]). Recursive partitioning, or classification tree analysis is a statistical method that splits, or partitions, data into smaller groups (nodes) of increasingly homogenous variance[42,43].

Descriptive statistics were performed on GraphPad Software (GraphPad Prism version 5.00 for Windows), and $p < 0.05$ was considered as significant (with $\alpha = 0.05$). To assess differences in THg concentrations, speciation, and isotopic values between sites, Kruskal-Wallis (K-W) tests were used, and Dunn's Multiple Comparison test (Dunn) was used to compare each pair of sites. Covariance between variables were evaluated using ANCOVA model on R [version 3.2.3]. Correlations between two variables were evaluated with Spearman's rank correlation coefficient (Spearman).

Physical parameters of the sampling sites (latitude, annual hours of sunshine and annual precipitation) were extracted from online database [44,45] and are detailed in Table S-5.

Table 1 : Age estimation, standard length (cm), body mass (g), THg and MeHg (ng·g^{-1}, dw), MeHg to THg ratio (%) trophic level, Hg isotopic ratios (as delta values, ‰) in muscle of *Dicentrarchus labrax*. All values are expressed as means ± standard deviation (SD), *(minimum-maximum)*, and n = number of analysed samples, except for age (only range is reported).

Sampling site (age range)	Std length	Body mass	[THg]	[MeHg]	% MeHg	Trophic level	δ^{202}Hg	Δ^{199}Hg	Δ^{201}Hg
AeS	28 ± 1	272 ± 48	598 ± 60	453 ± 51	90 ± 7	4.6 ± 0.3	-0.04 ± 0.08	0.81 ± 0.09	0.63 ± 0.09
Aegean Sea	*(25–30)*	*(205–380)*	*(511.2–685.1)*	*(369–527.6)*	*(71–95)*	*(4.3–5.1)*	*(-0.17– 0.07)*	*(0.68–0.95)*	*(0.49–0.78)*
(2 years)	n=10	n=10	n=10	n=10	n=10	n=10	n=10	n=10	n=10
NS	26 ± 6	192 ± 90	1139 ± 548	1025 ± 416	93 ± 3	5.5 ± 0.5	-0.06 ± 0.14	0.49 ± 0.03	0.32 ± 0.06
North Sea	*(16–31)*	*(43–278)*	*(347.7–1631)*	*(489–1396)*	*(89–95)*	*(4.8–5.9)*	*(-0.22 – 0.05)*	*(0.46–0.52)*	*(0.27–0.39)*
(1-3 years)	n=5	n=5	n=5	n=4	n=4	n=5	n=4	n=4	n=4
SE	33 ± 2	487 ± 66	1055 ± 218	988 ± 216	94 ± 1	4.6 ± 0.6	0.15 ± 0.14	0.37 ± 0.11	0.26 ± 0.07
Seine Estuary	*(30–35)*	*(350–563)*	*(658.5–1493)*	*(606.2–1427)*	*(93–94)*	*(4.1–6.1)*	*(-0.02–0.43)*	*(0.24–0.6)*	*(0.16–0.42)*
(3-4 years)	n=10	n=10	n=10	n=10	n=10	n=10	n=10	n=10	n=10
BS	21 ± 2	140 ± 24	102 ± 14	82 ± 11	83 ± 10	4.0 ± 0.1	0.14 ± 0.56	1.30 ± 0.16	1.03 ± 0.15
Black Sea	*(18–24)*	*(110–170)*	*(85.3–130.1)*	*(72.4–110.2)*	*(59–90)*	*(3.9–4.2)*	*(-0.77–1.11)*	*(0.98–1.48)*	*(0.74–1.17)*
(1-2)	n=10	n=10	n=10	n=10	n=10	n=10	n=10	n=10	n=10
NAS	22 ± 1	123 ± 20	1578 ± 1130	1137 ± 875	94 ± 2	5.5 ± 0.6	0.03 ± 0.09	0.53 ± 0.14	0.46 ± 0.15
Northern Adriatic Sea	*(20–23)*	*(89–149)*	*(596.3–3560)*	*(430–2677)*	*(92–97)*	*(4.6–6.3)*	*(-0.09– 0.17)*	*(0.4–0.87)*	*(0.23–0.74)*
(1 year)	n=9	n=9	n=9	n=9	n=9	n=9	n=9	n=9	n=9
RAR	21 ± 4	106 ± 60	809 ± 663	648 ± 534	91 ± 4	3.3 ± 0.8	0.14 ± 0.17	0.56 ± 0.14	0.46 ± 0.12
Ria de Aveiro Reference	*(17–26)*	*(55–217)*	*(143.2–2207)*	*(107–1858)*	*(83–95)*	*(2.4–4.7)*	*(-0.19 –0.4)*	*(0.31–0.74)*	*(0.31–0.61)*
(1-2 years)	n=10	n=10	n=10	n=10	n=10	n=10	n=10	n=10	n=10
RAC	17 ± 1	59 ± 10	1904 ± 282	1579 ± 249	94 ± 1	3.8 ± 0.4	0.32 ± 0.09	0.34 ± 0.08	0.26 ± 0.06
Ria de Aveiro Contaminated	*(16–18)*	*(45–77)*	*(1568–2411)*	*(1120–2046)*	*(91–96)*	*(3.3–4.6)*	*(0.1–0.45)*	*(0.22–0.49)*	*(0.15–0.34)*
(1 year)	n=12	n=12	n=12	n=12	n=12	n=12	n=12	n=12	n=12

3. Results

3.1 Fish comparability

Biometrical data of the fish are summarized in Table 1. Standard length and body mass varied significantly between sites (K-W; H = 52.15; p<0.0001 and H = 51.68; p<0.0001, respectively). Means of standard length and body mass were the smallest at RAC site and highest at SE site. Means for age were smallest for RAC and NAS and highest for SE site.

$\delta^{13}C$ values measured in muscles of seabass ranged from -24.9 ‰ to -14.5 ‰. The average value for the BS, -21.2 ‰, was lower than average values for all other locations (Dunn; p<0.05 for all locations except NAS, Table S-5 and Figure S-3). $\delta^{15}N$ values ranged between 10.5 ‰ and 21.1 ‰, means for each site are reported in Table S-5. Trophic levels (TL) were estimated in order to allow inter-site comparison and global correlations. The baseline $\delta^{15}N$ values used for each site, found in literature, are reported in Table S-7. TL varied between sites, (Figure S-4), with a minimum mean value at RAR site, and a maximum mean value at NAS and NS sites (Table 1).

3.2 Hg variables across sites

3.2.1 Total Hg concentration and speciation

THg concentrations in muscle sample of the seabass collected across Europe ranged between 85 $ng \cdot g^{-1}$ and 3560 $ng \cdot g^{-1}$ dry weight. Means were statistically different between sites (K-W; H = 46.07; p<0.0001; see Figure S-5). Mean THg concentration was lowest at BS site and highest at NAS and RAC sites (Table 1). All sampling sites except BS showed THg concentrations much higher than the environmental quality standard (EQS) of 20 $ng \cdot g^{-1}$ wet weight (WW) in fish, set by the European Water Framework Directive (WFD, EC, 2000), (corresponding to around 80 $ng \cdot g^{-1}$ DW in our samples). MeHg mean concentrations varied significantly between sampling sites (K-W: H = 46.76 ; p<0.0001). THg and MeHg were highly correlated (Spearman: r = 0.98 ; p<0.0001). MeHg represented around ≥

90% of the THg concentration for all sites, except BS site (83 ± 9%) whose %MeHg differed significantly from NS, SE, RAC and NAS (Figure S-6).

3.2.2 Hg stable isotopes

δ^{202}Hg means for each site ranged between -0.06 ± 0.14 ‰ at NS and 0.32 ± 0.09 ‰ at RAC (Table 1). δ^{202}Hg values differed significantly between sites (K-W; H = 25; p< 0.001; Figure S-7): RAC δ^{202}Hg median value differed significantly from AeS, NS and NAS (Dunn ; p<0.05). BS displayed the largest variation of δ^{202}Hg (1.8 ‰ between min and max). For this reason, we excluded BS from correlation tests on the whole data set.

All sites showed mass independent fractionation (MIF) of ^{199}Hg and ^{201}Hg (Table 1). A significant and strong correlation was observed between Δ^{199}Hg and Δ^{201}Hg (Figure S-8; Spearman; r = 0.95; p<0.0001), and value of the slope of the regression line was 1.20 ± 0.03. The slope of the regression line for each sampling site varied between 0.91 in AeS and 1.47 at SE (Figure S-9). An average Δ^{199}Hg of 0.34 ± 0.08 ‰ was measured at RAC site, which presented the lowest values of MIF, close to SE values, while highest MIF was measured at BS site with a mean of 1.30 ± 0.16 ‰. Δ^{199}Hg differed significantly between sampling sites (K-W; H = 51.02, p<0.0001; Figure S-7).

3.3 Discrimination of sampling sites

3.3.1 Hg isotopic niche using SIBER

SIBER analysis performed using MDF *versus* MIF values determined the core Hg isotopic niches of our 7 sampling sites (Figure 1). There was no overlap at all for the BS site, nor for the AeS site. There was little overlap between RAC and SE sites: 0.0036‰², which represents 7% and 15% of the SEA of SE

236 and RAC respectively. Finally, overlap between NAS, NS, RAR and SE was more important (>15%). The
237 area of the ellipse associated to BS site was the biggest (0.242 ‰²) while all the other sites had SEA
238 comprised between 0.019 and 0.080 ‰² (Figure S-10).
239

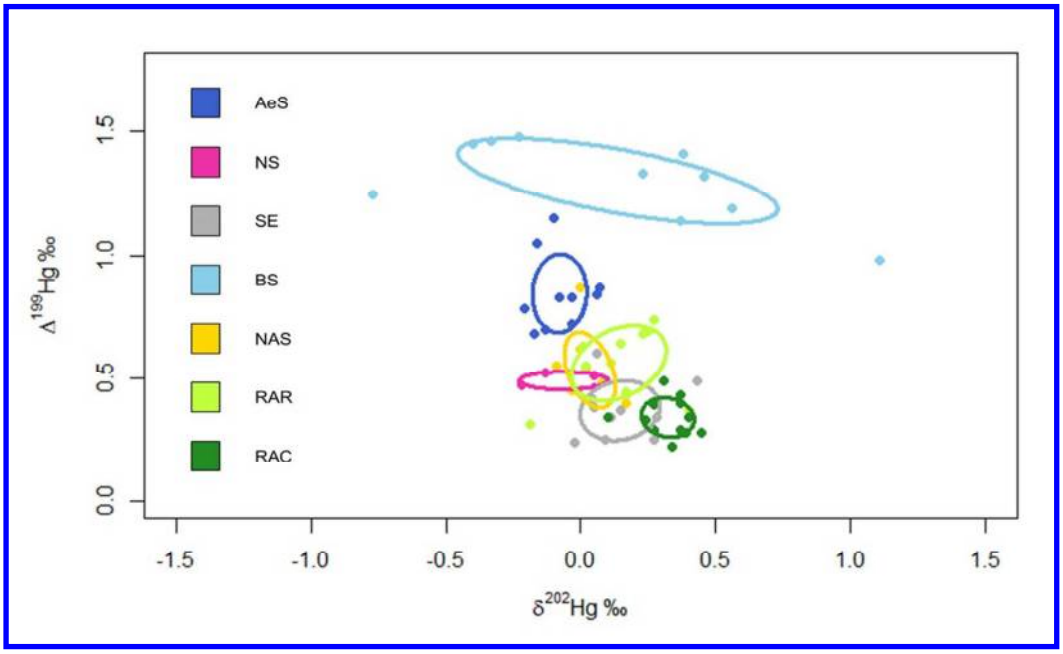

240

241 **Figure 1 :** Hg isotopic niches of *Dicentrarchus labrax* from 7 sampling sites across Europe: the Aegean Sea (AeS), the North
242 Sea (NS), the Seine estuary (SE), the Northern Adriatic Sea (NAS), the Black Sea (BS), and two different sites at the Ria de
243 Aveiro lagoon in Portugal: the reference site, RAR and the contaminated site RAC. Solid lines represent the bivariate
244 standard ellipses associated to each population (through SIBER). Dots represent each individual.
245

246 **3.3.2 Recursive partitioning**
247

248 Recursive partitioning analysis for Hg variables in populations of fish separated first the lowest THg
249 contaminated population (exclusively Black Sea (10/10) (<137 $ng.g^{-1}$ dw)) from the medium
250 contaminated (between 137 and 1530 $ng.g^{-1}$ dw) and the highest mercury contaminated population
251 (predominantly Ria de Aveiro Contaminated (12/12) and Northern Adriatic Sea (3/9)) (≥1530 $ng.g^{-1}$
252 dw). The medium THg contaminated group could then be discriminated by the $\Delta^{199}Hg$ values: higher
253 than 0.69 (predominantly Aegean Sea (10/10) and Ria de Aveiro Reference (3/10)), between 0.43 and

0.69 (predominantly Northern Adriatic Sea (5/9), Ria de Aveiro Reference (5/10) and North Sea (3/4)) and finally below 0.43 (predominantly Seine Estuary (8/10)) (Figure 2A). Classification error for this tree is between 30.8% and 43.1%. A second analysis focusing only on RAR, NAS and NS sites separated a group with higher δ^{202}Hg (≥ 0.095) (mainly RAR (6/10)) from the rest (Figure 2B).

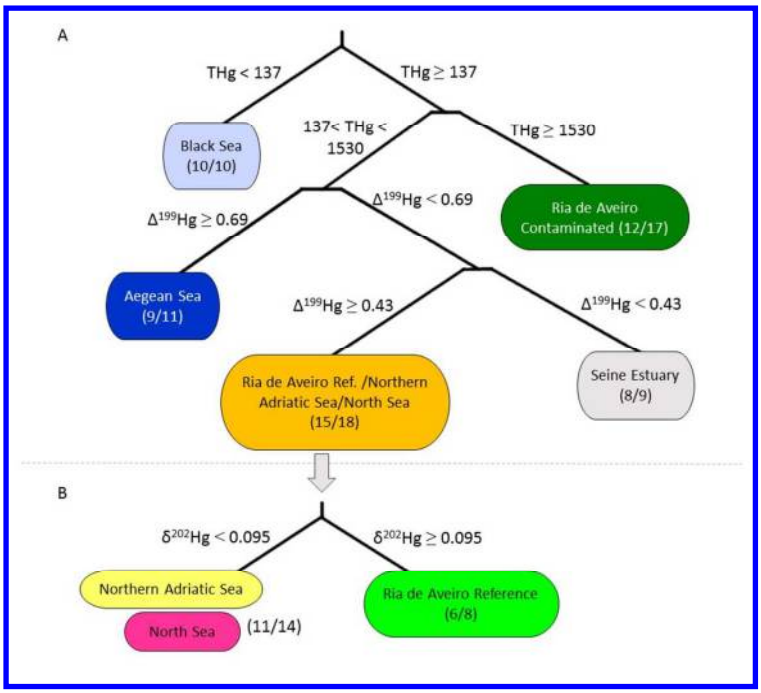

Figure 2 : (A) Classification tree for Hg variables in populations of *Dicentrarchus labrax*, after recursive partitioning analysis (n=65). This decision model has root node error of 0.82. (B) Classification tree performed only on Ria de Aveiro reference, North Sea and Northern Adriatic Sea populations (n=22).

3.4 Variables potentially related to MDF and MIF

3.4.1 Covariance of THg with biometrics and sites

We tested the effect of sampling site on mercury variables (Log(THg) and Log(MeHg)) with standard length + body mass + age + δ^{15}N + δ^{13}C + TL as covariates and interactions between covariates and sampling site. There was a significant effect of sampling site (ANCOVA: F = 47.0, df = 6.50, p<0.0001) and standard length (ANCOVA: F = 16.1, df = 1.50, p<0.0001) on THg, but the interaction between

sampling site and standard length was not significant (p>0.05). There was also a significant effect of sampling site (ANCOVA: F = 47.2, df =6.49, p<0.0001) and standard length (ANCOVA: F = 9.8, df = 1.49, p<0.0001) on MeHg, but the interaction between sampling site and standard length was not significant (p>0.05). The other tested covariates did not impact the results of THg and MeHg concentrations. Least-squares mean concentrations for each site when accounting for standard length are shown in SI, Table S-8 and S-9, and corroborate the ANCOVA analysis.

This means that THg and MeHg vary amongst sampling sites and that within sampling sites the standard length has an effect on mercury concentrations. But, the sampling site difference is independent from the standard length variation.

3.4.2 Correlations for δ^{202}Hg and Δ^{199}Hg

For whole data set, δ^{202}Hg was weakly correlated to THg (Spearman; r = 0.59; p<0.0001; Figure S-12), to MeHg (Spearman; r = 0.65; p<0.0001), and to TL (Spearman; r = -0.46; p<0.01). On the intra-population level, correlation could only be established in BS population between δ^{202}Hg and THg (Spearman; r = 0.77; p<0.01).

Δ^{199}Hg was negatively correlated with THg and MeHg concentrations (Spearman; r = -0,75 ; p < 0,0001 and r = -0.76 ; p < 0.0001). We plotted Δ^{199}Hg vs 1/THg to perform linear regression (Figure S-13). The R^2 of the regression line was higher for whole data set (0.69) than for the data set excluding BS and RAR values (0.43). No significant correlation could be observed between Δ^{199}Hg and TL or δ^{13}C.

3.4.3 Physical parameters

No significant correlation could be observed between Δ^{199}Hg and latitude, annual hours of sunshine and annual precipitation (Spearman; *p>0.05*). The correlation was performed on means for each site (n=7).

4. Discussion

4.1 Assessing the variability of Hg levels and possible links with diet

4.1.1 *THg and MeHg inter-site variability*

Interestingly, THg and MeHg concentrations in muscle were extremely variable between individual fish samples (from 85 to 3560 ng.g^{-1} dw Table 1 Figure S-5). The highest concentrations were observed in fish collected in NAS and RAC, two sites with a historical, industrial Hg contamination [21,32,46]. MeHg represented most of the THg found in seabass muscles. These data are consistent with previous studies that show that MeHg accumulates in fish muscle tissue where it typically comprises more than 90% of THg[15,26,47]. THg and MeHg concentrations in the muscle of teleost fish depend not only on the environmental contamination of their habitat, but also on several biotic factors including age, body mass, standard length, diet and trophic position in the food web[48–50]. However, the absence of association between mercury concentrations (THg and MeHg) and age, standard length or body mass indicated that these parameters did not explain the observed variability of THg and MeHg concentrations across sampling sites.

4.1.2 *MeHg levels related to the diet*

Diet is considered as the main source of MeHg in fish[51,52]. Understanding MeHg levels in fish therefore implies understanding their diet. Stomach content analyses (Table S-1) reveal a large panel of prey from small invertebrates to teleost fish, in agreement with previous published data describing the very opportunistic feeding behaviour of seabass[31]. The complexity and variability of regional food

webs can affect the relative trophic position [53] as well as the contamination level of seabass. Trophic level (TL), calculated using $\delta^{15}N$, varied between sampled populations (Figure S-4) and was positively correlated with standard length and body mass, which supports the idea that bigger fish occupy a higher trophic position. However, the lack of association between TL and THg or MeHg concentrations (taking into account the whole data set), indicated that if there is an effect of trophic position on Hg concentration in our data set, it is negligible.

$\delta^{13}C$ is commonly used to indicate the origin of carbon sources with a general pattern of coastal, benthos-linked food webs being more enriched in ^{13}C (higher $\delta^{13}C$) compared to offshore, pelagic food webs[54]. The $\delta^{13}C$ values measured in AeS, NS, SE, NAS, RAC and RAR were in agreement with values reported previously for seabass [55–59]. $\delta^{13}C$ values measured in BS fish samples were lower than in other sampling sites and were concordant with values reported in other biota from the Black Sea[60,61]. The lower $\delta^{13}C$ values found in BS population suggest a more offshore-based food web than other sampling sites food webs. However, as BS site is the only one to stand out via $\delta^{13}C$, it is likely that all other sites have similarly rooted food webs. As THg was not associated to $\delta^{13}C$, this tool does not explain the variation of mercury concentrations between sites.

All the sampling sites in this study were located in coastal areas. However, they presented different environmental characteristics (shelf, shore, lagoon, estuary) and different anthropogenic contexts. Our analyses show that the two sites directly influenced by industrial or mining effluent containing high levels of mercury, NAS and RAC, house the two most contaminated fish populations.

Therefore, we suggest that ecosystem-related differences such as site contamination levels, are likely the best explanation to the observed variability of THg and MeHg concentrations between sites.

4.1.3 The Black Sea specificities

Many parameters measured in fish from the Black Sea suggest the peculiarity of Hg sources and cycling in this site. First, there is the low Hg concentrations (102 $ng \cdot g^{-1}$ dry weight) associated with a

lower %MeHg in muscles (80% instead of the usual above 90%). Lower Hg levels have previously been described in BS organisms and attributed to the special hydrological conditions in BS (mainly considered to be a sink for particulate organic matter and its pollutant load)[60,62]. MeHg concentrations in waters of the BS have been reported to be as high as in the Mediterranean[63], but the BS is subject to massive eutrophication and subsequent increase of nitrates and phosphates[64–66]. This could result in a rise of primary production and a decrease of Hg methylation, consequently diluting THg concentration in phytoplankton and diminishing MeHg concentration in water and biota[67]. Other studies have shown that the relative contribution of inorganic Hg vs MeHg to the overall Hg bioaccumulation is largely controlled by the relative concentration of MeHg dissolved in seawater[68]. The high concentration of organic matter in BS could result in a strong complexation of IHg, making it less available for methylation [69]. Our results seem to correspond to such a situation where MeHg is proportionally less abundant compared to IHg in waters of the Black Sea than in all other sampling sites.

4.2 European seabass populations discrimination by Hg isotopes

4.2.1 Do $\Delta^{199}Hg$ and $\delta^{202}Hg$ of seabass populations around Europe vary?

The SIBER plot of MDF (δ^{202}Hg) versus MIF ($\Delta^{199}Hg$) values measured in the muscle of seabass allows for the discrimination of several sampling sites (Figure 1). Four groups could be distinguished based on their core isotopic niche. On one side, clearly apart because of higher Δ^{199}Hg (MIF axis), stands the BS site. The MIF axis also enables us to discriminate the AeS site from a group of more heavily contaminated sites (NS, SE, NAS, RAR), displaying low Δ^{199}Hg and δ^{202}Hg. Eventually, the MDF axis (δ^{202}Hg) sets RAC site slightly apart.

The δ^{202}Hg and Δ^{199}Hg values are in the range of previously published data in marine fish[15,26,70] (Figure S-14), and constitute, to our knowledge, the first data for European coastal fish.

374

375 *4.2.2 Are Hg stable isotopes useful to discriminate seabass populations?*

376 In order to better test whether δ^{202}Hg and Δ^{199}Hg effectively enables the discrimination of different
377 populations of fish, we used classification tree analysis (Figure 2 and Figure S-11). The variables THg
378 and Δ^{199}Hg enabled the discrimination of different populations of fish. The recursive partitioning
379 analysis for Hg variables partitioned our 7 populations into 5 groups (Figure 2A). AeS, BS, RAC and SE
380 sites could be well discriminated. The fifth group was quite heterogeneous, associating fish from NAS
381 with those from RAR and NS. Due to the classification into 5 groups instead of 7, the predictive
382 power of this tree is relatively moderate (classification error between 30.8% and 43.1%). But If RAR,
383 NAS and NS are artificially grouped, the classification error decreases down to 16%. A second analysis
384 (Figure 2B) focusing only on the 3 groups that could not be discriminated by the first analysis further
385 enabled the discrimination of the RAR site from the NS and NAS with the variable δ^{202}Hg.

386

387 The need to combine MDF and MIF values with THg to obtain a better classification does not
388 contradict their discriminating power because the recursive-partitioning still needs δ^{202}Hg and Δ^{199}Hg
389 to build the classification tree. Thus, we conclude that both δ^{202}Hg and Δ^{199}Hg allow for the successful
390 discrimination of several populations of fish from different areas across Europe. The combination of
391 MDF and MIF values increases their discriminating power, and their combination with THg
392 concentrations increases their discriminating power even more.

393

394 ***4.3*** **MIF of Hg in seabass to assess Hg sources in coastal areas**

395

396 MIF varied significantly between sampling sites (Figure S-7B). We found a Δ^{199}Hg/Δ^{201}Hg slope of
397 1.20, which is in accordance with the slopes reported in other marine fish (~ 1.2) exposed to
398 photodegraded MeHg from their respective environment [15,26,28,70,71]. Hence, in the present study, MIF
399 values measured in fish muscles are assumed to directly reflect the accumulation of residual MeHg

after demethylation, before it enters the food web. Yet, we could not find any correlation with latitude, hours of light per year, or precipitation (factors that could influence demethylation rates). The absence of correlation between MIF and TL is probably related to the relatively constant %MeHg from one site to another.

The positive correlation between MIF and 1/THg (Figure S-13) is in accordance with findings from other studies[15,21,22] where various contaminated sites have been characterized by (close to) zero Δ^{199}Hg values. As MIF of Hg in fish is the result of the photodemethylation of MeHg, positive Δ^{199}Hg values may be imparted in less contaminated sites that lack significant inputs from anthropogenic Hg sources, such as BS and AeS. Meanwhile, Δ^{199}Hg closer to 0 ‰, associated with higher THg and MeHg concentrations (*e.g.* in SE and RAC), reflects more the impact of anthropogenic Hg in these sites, related to a dilution of the demethylation footprint and/or related to the higher contribution of continental and benthic input of MeHg (which would display low MIF). The mild correlation between MIF and MeHg (r^2=0.58) could indicate that other factors than THg and MeHg concentrations play an important role in MIF. However the finding that MIF trend is following a general decrease down to value close to 0 when all the sites are compiled together demonstrates that such isotopic composition could be further used to establish a clear impact of coastal Hg pollution to juvenile seabass population, in opposition to what is observed for more pelagic species and environments. (Further discussion available in SI)

BS MIF values (Δ^{199}Hg= 1.30 ‰) were similar to values measured both in coastal fish[70] and in oceanic tuna[26] (Figure S-14). Our samples are coastal, but there exists indications of a rather pelagic-rooted Hg source, *i.e.* the lower δ^{13}C compared to other sites (-21.2 ‰). Another explanation for higher MIF values could be linked to special features of the BS: it is a land-locked sea receiving loads of freshwater inputs that cause substantial eutrophication and relatively low salinity of surface layer waters [64,72]. Now, it has been observed that MIF levels are significantly higher in freshwater lakes

than in marine waters[16,25,26,73]. Although the mechanisms behind these observations are still unclear, previous studies suggest that it is likely the consequence of the accumulation of MeHg that undergoes more photodegradation because of lower salinity and maybe higher dissolved organic carbon (DOC)[73]. Hence, analogy with Black Sea characteristics can be made, that could partly explain the relatively high MIF values found there. Paradoxically, the $\Delta^{199}Hg/\Delta^{201}Hg$ slope (Figure S-9) rather pleads in favour of MIF originating from the photoreduction of IHg. As the BS samples display a lower %MeHg than other sites, the influence of IHg on the overall MIF measured in seabass could be more pronounced. Besides, this would be coherent with our previous assumption that IHg concentration is proportionally more abundant compared to MeHg in waters of the Black Sea than in all other sampling locations in this study.

Moreover, $\delta^{202}Hg$ absolute values in BS were consistent with previous studies on freshwater biota[16,25,73], corroborating the MIF results interpretation.

Thus, our study shows that $\Delta^{199}Hg$ in a predatory fish reflects the level of contamination of fish in relation to the Hg pollution of their coastal habitat. Beside, MIF can also be influenced by specific ecological characteristics, and therefore used to identify and investigate peculiar Hg environments such as in the Black Sea.

4.4 MDF of Hg in seabass to asses major Hg sources in coastal areas

$\delta^{202}Hg$ did not vary significantly between sites except for RAC site, which showed an enrichment with heavier Hg isotope relative to all other sites but BS (Figure S-7A). Overall, Hg stable isotopic ratios displayed a wide range of values among samples ($\delta^{202}Hg$ from -0.77 ‰ to 1.11 ‰), that are consistent with other studies on marine organisms[15,26,70] except for the highest values that

451 correspond more to data published for fresh water biota[16,25,73]. When BS values are excluded, the
452 δ^{202}Hg range goes from -0.22 to 0.45 ‰, representing a variation of only 0.67 ‰.
453
454 *4.3.1 MDF of Hg: about the influence of trophic relationships*
455 Processes responsible for MDF are microbially mediated reduction or methylation of inorganic
456 Hg(II)[74], degradation of MeHg[19], and abiotic, physical and photochemical transformations of both IHg
457 and MeHg[16]. *In vivo* processes and trophic transfer may also influence MDF[16,75], but the question
458 remains debatable because of previous and non-conclusive studies on fish feeding experiments
459 [27,76,77]. In the present study, no correlation between δ^{202}Hg and δ^{15}N (reflecting trophic position),
460 MeHg concentration or %MeHg could be observed on the intra-population level. Hence, this study
461 suggests no evidence of significant MDF caused by trophic transfer and we can consider that it might
462 be negligible in the case of juvenile seabass.
463
464 The wide range of δ^{202}Hg values in BS site (total range of 1.88 ‰) is not comparable to any range
465 described for a single species fish population elsewhere in literature[15,16,26,73,75], and could be linked to
466 *in vivo* processes (further discussion in SI).
467
468 *4.3.2 MDF providing clues on Hg sources*
469
470 The increase of δ^{202}Hg with THg (Figure S-12) suggests that there could be a background δ^{202}Hg signal
471 that is gradually replaced by a contamination-related δ^{202}Hg. A recent study in Arctic coastal
472 seawaters, which is a relatively pristine environment, showed negative δ^{202}Hg in waters (-2.85 to -
473 1.10 ‰) and sediments (-0.76 ‰) [78]. These negative values could constitute a good indication of
474 background contamination δ^{202}Hg, most probably related to atmospheric deposition and are
475 coherent with our results.
476

Indeed, in previous studies on marine environment, the extent of the isotopic δ^{202}Hg offset between sediment THg and fish THg was estimated around 0.73 ‰ (± 0.16 ‰ 1SD)[70] and 0.66 ‰(± 0.25 ‰ 1SD)[15]. If we consider that there is similar δ^{202}Hg offset between fish and sediment in AeS, the δ^{202}Hg in sediment is estimated around -0.74 ‰. This is consistent with background sediment δ^{202}Hg found in arctic coastal waters [78]. The negative δ^{202}Hg (-0.04 ‰) measured in the least contaminated site, AeS, would thus be related to background Hg isotopic composition.

At the other end of the δ^{202}Hg gradient (Figure S-12), the RAC site (and the SE and NAS sites to a lesser extent) showed a higher δ^{202}Hg that would be more related to the local contamination. δ^{202}Hg of RAC site (mean= 0.32 ‰) is higher than all other sites (Figure S-7A). RAC site is acknowledged as a heavily polluted area[32,79] that was subjected to Hg effluents from a chlor-alkali plant. The chlor-alkali process uses liquid elemental Hg as a catalyst to produce NaOH, and there are evidences of large losses of Hg with waste water, contaminating local sediments around industries[12]. RAC site is indeed the site displaying the highest THg and MeHg mean concentrations in this study. Chlor-alkali processes induce MDF, sometimes to a large extent[12] and the imprint of the processes on the Hg waste has been shown to be reflected in contaminated local sediments[12]. Hence, we suggest that higher δ^{202}Hg observed at RAC site is to be linked with the isotopic composition of the contamination source, from chlor-alkali industry waste, mainly as elemental Hg.

It is interesting to note that overall, δ^{202}Hg varies little between sites (means range between -0.06 and 0.15 ‰, RAC excluded). Worldwide and in Europe, around 80% of Hg emission comes from combustion, releasing Hg into the atmosphere[4]. Therefore, it would be plausible that a global atmospheric pollution affects all our sampling sites, mitigating the δ^{202}Hg value from local contamination sources and leading to some homogenization of δ^{202}Hg values across our sampling sites. In a context of global atmospheric Hg contamination, RAC site δ^{202}Hg would stand out because the local industrial contamination source would be particularly important and the dominant Hg

source, with a δ^{202}Hg composition clearly different from that of the global source. At the opposite, AeS, the least contaminated site probably represents a δ^{202}Hg much closer to background/atmospheric contamination, meanwhile sites such as SE and NAS represent intermediate δ^{202}Hg values. Full discussion about SE, NAS, and RAR sites are available in SI.

Overall, our results thus indicate that Hg isotopes can indeed help discriminating local versus global contamination. They bring out the possibility to use Hg stable isotopes to identify particularities in the Hg cycle of several local sites (like the BS and RAC), to discriminate distinct populations and to explore the Hg cycle on a large scale, namely Europe.

5. Acknowledgements

Alice Cransveld acknowledges a PhD F.R.I.A. grant (F.R.S-FNRS). Krishna Das is a Senior F.R.S.-FNRS Research Associate (Fond pour la Recherche Scientifique). Cláudia Mieiro acknowledges the Portuguese Foundation for Science and Technology (FCT) (grant SFRH/BPD/100740/2014). The authors warmly thank Renzo Biondo and Caiyan Feng, L. Michel and F. Remy. The study received funding of Research Council of ULiège (FSRC-13/82).

Supporting information. Additional data, figures, tables, methodology, and discussion.

References

(1) National Research Council; Comittee on the toxicological effects of Methylmercury; Board on Environmental Studies and Toxicology. *Toxicological effects of methylmercury*; National Academy Press: Washington DC, 2000.

(2) Boening, D. W. Ecological effects, transport, and fate of mercury: a general review. *Chemosphere* **2000**, *40* (12), 1335–1351.

(3) OSPAR Commission. *Quality status report 2010*; The Commission, 2010.

(4) UNEP. *Global Mercury Assessment 2013: Sources, Emissions, Releases and Environmental Tansport*; Geneva, Switzerland, 2013.

(5) Storelli, M. M.; Giacominelli-Stuffler, R.; Marcotrigiano, G. Mercury accumulation and speciation in muscle tissue of different species of sharks from Mediterranean Sea, Italy. *Bull. Environ. Contam. Toxicol.* **2002**, *68* (2), 201–210.

(6) Storelli, M. M.; Ceci, E.; Storelli, A.; Marcotrigiano, G. O. Polychlorinated biphenyl, heavy metal and methylmercury residues in hammerhead sharks: contaminant status and assessment. *Mar. Pollut. Bull.* **2003**, *46* (8), 1035–1039.

(7) Storelli, M. M.; Storelli, A.; Giacominelli-Stuffler, R.; Marcotrigiano, G. O. Mercury speciation in the muscle of two commercially important fish, hake (*Merluccius merluccius*) and striped mullet (*Mullus barbatus*) from the Mediterranean sea: estimated weekly intake. *Food Chem.* **2005**, *89* (2), 295–300.

(8) Habran, S.; Debier, C.; Crocker, D. E.; Houser, D. S.; Das, K. Blood dynamics

of mercury and selenium in northern elephant seals during the lactation period. *Environ. Pollut.* **2011**, *159* (10), 2523–2529.

(9) Das, K.; Siebert, U.; Gillet, A.; Dupont, A.; Di-Poï, C.; Fonfara, S.; Mazzucchelli, G.; De Pauw, E.; De Pauw-Gillet, M. C. Mercury immune toxicity in harbour seals: links to in vitro toxicity. *Environ. Heal.* **2008**, *7* (1), 52.

(10) Bergquist, B. A.; Blum, J. D. The odds and evens of mercury isotopes: Applications of mass-dependent and mass-independent isotope fractionation. *Elements* **2009**, *5* (6), 353–357.

(11) Lin, C. J.; Singhasuk, P.; Pehkonen, S. O. *Environmental Chemistry and Toxicology of Mercury*; Liu, G., Cai, Y., O'Driscoll, N., Eds.; John Wiley & Sons, Inc.: Hoboken, NJ, USA, 2011.

(12) Wiederhold, J. G.; Skyllberg, U.; Drott, A.; Jiskra, M.; Jonsson, S.; Björn, E.; Bourdon, B.; Kretzschmar, R. Mercury isotope signatures in contaminated sediments as a tracer for local industrial pollution sources. *Environ. Sci. Technol.* **2015**, *49* (1), 177–185.

(13) Blum, J. D.; Popp, B. N.; Drazen, J. C.; Anela Choy, C.; Johnson, M. W. Methylmercury production below the mixed layer in the North Pacific Ocean. *Nat. Geosci* **2013**, *6* (10), 879–884.

(14) Fitzgerald, W. F.; Lamborg, C. H.; Hammerschmidt, C. R. Marine biogeochemical cycling of mercury. *Chem. Rev.* **2007**, *107* (2), 641–662.

(15) Kwon, S. Y.; Blum, J. D.; Chen, C. Y.; Meattey, D. E.; Mason, R. P. Mercury Isotope Study of Sources and Exposure Pathways of Methylmercury in Estuarine Food Webs in the Northeastern U.S. *Environ. Sci. Technol.* **2014**, *48* (17), 10089–10097.

(16) Bergquist, B. A.; Blum, J. D. Mass-dependent and-independent fractionation of Hg isotopes by photoreduction in aquatic systems. *Science (80-.).* **2007**, *318* (5849), 417–420.

(17) Blum, J. D.; Bergquist, B. A. Reporting of variations in the natural isotopic composition of mercury. *Anal. Bioanal. Chem.* **2007**, *388* (2), 353–359.

(18) Rodŕiguez-Gonźalez, P.; Epov, V. N.; Bridou, R.; Tessier, E.; Guyoneaud, R.; Monperrus, M.; Amouroux, D. Species-specific stable isotope fractionation of mercury during Hg(II) methylation by an anaerobic bacteria (*Desulfobulbus propionicus*) under dark conditions. *Environ. Sci. Technol.* **2009**, *43* (24), 9183–9188.

(19) Kritee, K.; Barkay, T.; Blum, J. D. Mass dependent stable isotope fractionation of mercury during mer mediated microbial degradation of monomethylmercury. *Geochim. Cosmochim. Acta* **2009**, *73* (5), 1285–1296.

(20) Chen, C. Y.; Borsuk, M. E.; Bugge, D. M.; Hollweg, T.; Balcom, P. H.; Ward, D. M.; Williams, J.; Mason, R. P. Benthic and Pelagic Pathways of Methylmercury Bioaccumulation in Estuarine Food Webs of the Northeast United States. *PLoS One* **2014**, *9* (2), e89305.

(21) Foucher, D.; Hintelmann, H. Tracing mercury contamination from the Idrija mining region (Slovenia) to the Gulf of Trieste using Hg isotope ratio measurements. *Environ. Sci. Technol.* **2008**, *43* (1), 33–39.

(22) Gehrke, G. E.; Blum, J. D.; Marvin-DiPasquale, M. Sources of mercury to San Francisco Bay surface sediment as revealed by mercury stable isotopes. *Geochim. Cosmochim. Acta* **2011**, *75* (3), 691–705.

(23) Sherman, L. S.; Blum, J. D.; Dvonch, J. T.; Gratz, L. E.; Landis, M. S. The use

595 of Pb, Sr, and Hg isotopes in Great Lakes precipitation as a tool for pollution
596 source attribution. *Sci. Total Environ.* **2015**, *502*, 362–374.

597 (24) Laffont, L. Fractionnement des isotopes stables de mercure dans un
598 écosystème tropical en Amazonie bolivienne et dans les cheveux de
599 populations humaines exposées, Université de Toulouse, Université Toulouse
600 III-Paul Sabatier, 2009.

601 (25) Gantner, N.; Hintelmann, H.; Zheng, W.; Muir, D. C. Variations in stable isotope
602 fractionation of Hg in food webs of arctic lakes. *Environ. Sci. Technol.* **2009**, *43*
603 (24), 9148–9154.

604 (26) Senn, D. B.; Chesney, E. J.; Blum, J. D.; Bank, M. S.; Maage, A.; Shine, J. P.
605 Stable isotope (N, C, Hg) study of methylmercury sources and trophic transfer
606 in the Northern Gulf of Mexico. *Environ. Sci. Technol.* **2010**, *44* (5), 1630–1637.

607 (27) Kwon, S. Y.; Blum, J. D.; Chirby, M. A.; Chesney, E. J. Application of mercury
608 isotopes for tracing trophic transfer and internal distribution of mercury in
609 marine fish feeding experiments. *Environ. Toxicol. Chem.* **2013**, *32* (10), 2322–
610 2330.

611 (28) Day, R. D.; Roseneau, D. G.; Berail, S.; Hobson, K. A.; Donard, O. F. X.;
612 Vander Pol, S. S.; Pugh, R. S.; Moors, A. J.; Long, S. E.; Becker, P. R. Mercury
613 Stable Isotopes in Seabird Eggs Reflect a Gradient from Terrestrial Geogenic
614 to Oceanic Mercury Reservoirs. *Environ. Sci. Technol.* **2012**, *46* (10), 5327–
615 5335.

616 (29) Loizeau, V.; Abarnou, A.; Ménesguen, A. A steady-state model of PCB
617 bioaccumulation in the seabass (*Dicentrarchus labrax*) food web from the
618 Seine estuary, France. *Estuaries and Coasts* **2001**, *24* (6), 1074–1087.

(30) Schnitzler, J. G.; Thomé, J. P.; Lepage, M.; Das, K. Organochlorine pesticides, polychlorinated biphenyls and trace elements in wild European seabass (*Dicentrarchus labrax*) off European estuaries. *Sci. Total Environ.* **2011**, *409* (19), 3680–3686.

(31) Pickett, G. D.; Pawson, M. G. *Seabass: biology, exploitation and conservation*; Springer, 1994; Vol. 12.

(32) Coelho, J. P.; Pereira, M. E.; Duarte, A.; Pardal, M. A. Macroalgae response to a mercury contamination gradient in a temperate coastal lagoon (Ria de Aveiro, Portugal). *Estuar. Coast. Shelf Sci.* **2005**, *65* (3), 492–500.

(33) Maury-Brachet, R.; Durrieu, G.; Dominique, Y.; Boudou, A. Mercury distribution in fish organs and food regimes: Significant relationships from twelve species collected in French Guiana (Amazonian basin). *Sci. Total Environ.* **2006**, *368* (1), 262–270.

(34) Fritsch, M. Traits biologiques et exploitation du bar commun Dicentrarchus labrax (L.) dans les pêcheries françaises de la Manche et du golfe de Gascogne, Université de Bretagne Occidentale, 2005.

(35) Remy, F.; Darchambeau, F.; Melchior, A.; Lepoint, G. Impact of food type on respiration, fractionation and turnover of carbon and nitrogen stable isotopes in the marine amphipod Gammarus aequicauda (Martynov, 1931). *J. Exp. Mar. Bio. Ecol.* **2017**, *486*, 358–367.

(36) Post, D. M. Using stable isotopes to estimate trophic position: models, methods, and assumptions. *Ecology* **2002**, *83* (3), 703–718.

(37) Habran, S.; Crocker, D. E.; Debier, C.; Das, K. How are trace elements mobilized during the postweaning fast in Northern elephant seals? *Environ.*

643 *Toxicol. Chem.* **2012**, *31* (10), 2354–2365.

644 (38) Rodríguez Martín-Doimeadios, R. C.; Krupp, E.; Amouroux, D.; Donard, O. F.
645 X. Application of Isotopically Labeled Methylmercury for Isotope Dilution
646 Analysis of Biological Samples Using Gas Chromatography/ICPMS. *Anal.*
647 *Chem.* **2002**, *74* (11), 2505–2512.

648 (39) Jackson, A. L.; Inger, R.; Parnell, A. C.; Bearhop, S. Comparing isotopic niche
649 widths among and within communities: SIBER - Stable Isotope Bayesian
650 Ellipses in R. *J. Anim. Ecol.* **2011**, *80* (3), 595–602.

651 (40) Therneau, T. M.; Atkinson, B. R port by Brian Ripley. rpart: Recursive
652 Partitioning, R. 2011.

653 (41) Team, R. C. R: A language and environment for statistical computing. Vienna,
654 Austria: R Foundation for Statistical Computing; 2014. 2014.

655 (42) Strobl, C.; Malley, J.; Tutz, G. An introduction to recursive partitioning:
656 rationale, application, and characteristics of classification and regression trees,
657 bagging, and random forests. *Psychol. Methods* **2009**, *14* (4), 323.

658 (43) Zhang, H. Recursive partitioning and tree-based methods. In *Handbook of*
659 *computational statistics*; Springer, 2012; pp 853–882.

660 (44) Climate Europe www.climatedata.eu (accessed Mar 13, 2015).

661 (45) Canty, J.; Frischling, B.; Frischling, D. Weatherbase www.weatherbase.com
662 (accessed Mar 13, 2015).

663 (46) Acquavita, A.; Covelli, S.; Emili, A.; Berto, D.; Faganeli, J.; Giani, M.; Horvat,
664 M.; Koron, N.; Rampazzo, F. Mercury in the sediments of the Marano and
665 Grado Lagoon (northern Adriatic Sea): Sources, distribution and speciation.
666 *Estuar. Coast. Shelf Sci.* **2012**, *113*, 20–31.

667 (47) Bloom, N. S. On the Chemical Form of Mercury in Edible Fish and Marine
668 Invertebrate Tissue. *J. Can. des Sci. halieutiques Aquat.* **1992**, *49* (5), 1010–
669 1017.

670 (48) Trudel, M.; Rasmussen, J. B. Bioenergetics and mercury dynamics in fish: a
671 modelling perspective. *Can. J. Fish. Aquat. Sci.* **2006**, *63* (8), 1890–1902.

672 (49) Kidd, K.; Clayden, M.; Jardine, T. Bioaccumulation and biomagnification of
673 mercury through food webs. *Environ. Chem. Toxicol. Mercur. Wiley, Hoboken*
674 **2012**, 455–499.

675 (50) Scheuhammer, A. M.; Meyer, M. W.; Sandheinrich, M. B.; Murray, M. W.
676 Effects of Environmental Methylmercury on the Health of Wild Birds, Mammals,
677 and Fish. *AMBIO A J. Hum. Environ.* **2007**, *36* (1), 12–19.

678 (51) Mason, R. P.; Laporte, J. M.; Andres, S. Factors Controlling the
679 Bioaccumulation of Mercury, Methylmercury, Arsenic, Selenium, and Cadmium
680 by Freshwater Invertebrates and Fish. *Arch. Environ. Contam. Toxicol.* **2000**,
681 *38* (3), 283–297.

682 (52) Hrenchuk, L. E.; Blanchfield, P. J.; Paterson, M. J.; Hintelmann, H. H. Dietary
683 and Waterborne Mercury Accumulation by Yellow Perch: A Field Experiment.
684 *Environ. Sci. Technol.* **2011**, *46* (1), 509–516.

685 (53) Lorrain, A.; Graham, B. S.; Popp, B. N.; Allain, V.; Olson, R. J.; Hunt, B. P. V.;
686 Potier, M.; Fry, B.; Galván-Magaña, F.; Menkes, C. E. R.; et al. Nitrogen
687 isotopic baselines and implications for estimating foraging habitat and trophic
688 position of yellowfin tuna in the Indian and Pacific Oceans. *Deep Sea Res. Part*
689 *II Top. Stud. Oceanogr.* **2015**, *113*, 188–198.

690 (54) Hobson, A. K. Tracing origins and migration of wildlife using stable isotopes: a

691 review. *Oecologia* **1999**, *120* (3), 314–326.

692 (55) França, S.; Vasconcelos, R. P.; Tanner, S.; Máguas, C.; Costa, M. J.; Cabral,
693 H. N. Assessing food web dynamics and relative importance of organic matter
694 sources for fish species in two Portuguese estuaries: a stable isotope
695 approach. *Mar. Environ. Res.* **2011**, *72* (4), 204–215.

696 (56) Pasquaud, S.; Elie, P.; Jeantet, C.; Billy, I.; Martinez, P.; Girardin, M. A
697 preliminary investigation of the fish food web in the Gironde estuary, France,
698 using dietary and stable isotope analyses. *Estuar. Coast. Shelf Sci.* **2008**, *78*
699 (2), 267–279.

700 (57) Barnes, C.; Jennings, S.; Polunin, N. V. C.; Lancaster, J. E. The importance of
701 quantifying inherent variability when interpreting stable isotope field data.
702 *Oecologia* **2007**, *155* (2), 227–235.

703 (58) Jennings, S.; van der Molen, J. Trophic levels of marine consumers from
704 nitrogen stable isotope analysis: estimation and uncertainty. *ICES J. Mar. Sci.*
705 *J. du Cons.* **2015**, *72* (8), 2289–2300.

706 (59) Spitz, J.; Chouvelon, T.; Cardinaud, M.; Kostecki, C.; Lorance, P. Prey
707 preferences of adult seabass *Dicentrarchus labrax* in the northeastern Atlantic:
708 implications for bycatch of common dolphin *Delphinus delphis*. *ICES J. Mar.*
709 *Sci.* **2013**, *70* (2), 452–461.

710 (60) Das, K.; Holsbeek, L.; Browning, J.; Siebert, U.; Birkun, A.; Bouquegneau, J.-
711 M. Trace metal and stable isotope measurements (delta13C and delta15N) in
712 the harbour porpoise *Phocoena phocoena relicta* from the Black Sea. *Environ.*
713 *Pollut.* **2004**, *131* (2), 197–204.

714 (61) Çoban-Yıldız, Y.; Altabet, M. A.; Yılmaz, A.; Tuğrul, S. Carbon and nitrogen

isotopic ratios of suspended particulate organic matter (SPOM) in the Black Sea water column. *Deep Sea Res. Part II Top. Stud. Oceanogr.* **2006**, *53* (17–19), 1875–1892.

(62) Joiris, C. R.; Holsbeek, L.; Bolba, D.; Gascard, C.; Stanev, T.; Komakhidze, A.; Baumgärtner, W.; Birkun, A. Total and Organic Mercury in the Black Sea Harbour Porpoise *Phocoena phocoena relicta*. *Mar. Pollut. Bull.* **2001**, *42* (10), 905–911.

(63) Harmelin-Vivien, M.; Cossa, D.; Crochet, S.; Bănaru, D.; Letourneur, Y.; Mellon-Duval, C. Difference of mercury bioaccumulation in red mullets from the north-western Mediterranean and Black seas. *Mar. Pollut. Bull.* **2009**, *58* (5), 679–685.

(64) Akbal, F.; Gürel, L.; Bahadır, T.; Güler, İ.; Bakan, G.; Büyükgüngör, H. Water and sediment quality assessment in the mid-Black Sea coast of Turkey using multivariate statistical techniques. *Environ. Earth Sci.* **2011**, *64* (5), 1387–1395.

(65) Sorokin, Y. U. I. The Black Sea. In *Etuaries and Enclosed Seas: Ecosystems of the World*; Elsevier, Ed.; Amsterdam, 1983; pp 253–291.

(66) Lamborg, C. H.; Yiğiterhan, O.; Fitzgerald, W. F.; Balcom, P. H.; Hammerschmidt, C. R.; Murray, J. Vertical distribution of mercury species at two sites in the Western Black Sea. *Mar. Chem.* **2008**, *111* (1–2), 77–89.

(67) Driscoll, C. T.; Chen, C. Y.; Hammerschmidt, C. R.; Mason, R. P.; Gilmour, C. C.; Sunderland, E. M.; Greenfield, B. K.; Buckman, K. L.; Lamborg, C. H. Nutrient supply and mercury dynamics in marine ecosystems: A conceptual model. *Env. Res* **2012**, *119*, 118–131.

(68) Wang, W. X.; Wong, R. S. K. Bioaccumulation kinetics and exposure pathways

739 of inorganic mercury and methylmercury in a marine fish, the sweetlips
740 *Plectorhinchus gibbosus*. *Mar. Ecol. Prog. Ser.* **2003**, *261*, 257–268.

741 (69) Lin, C.-C.; Yee, N.; Barkay, T. Microbial transformations in the mercury cycle.
742 *Environ. Chem. Toxicol. Mercur.* **2012**, 155–191.

743 (70) Gehrke, G. E.; Blum, J. D.; Slotton, D. G.; Greenfield, B. K. Mercury Isotopes
744 Link Mercury in San Francisco Bay Forage Fish to Surface Sediments. *Environ.*
745 *Sci. Technol.* **2011**, *45* (4), 1264–1270.

746 (71) Point, D.; Sonke, J. E.; Day, R. D.; Roseneau, D. G.; Hobson, K. A.; Vander
747 Pol, S. S.; Moors, A. J.; Pugh, R. S.; Donard, O. F. X.; Becker, P. R.
748 Methylmercury photodegradation influenced by sea-ice cover in Arctic marine
749 ecosystems. *Nat. Geosci.* **2011**, *4* (3), 188–194.

750 (72) Borysova, O.; Kondakov, A.; Paleari, S.; Rautalahti-Miettinen, E.; Stolberg, F.;
751 Daler, D. *Eutrophication in the Black Sea region; Impact assessment and*
752 *Causal chain analysis*; Kalmar, Sweden, 2005.

753 (73) Perrot, V.; Pastukhov, M. V; Epov, V. N.; Husted, S.; Donard, O. F. X.;
754 Amouroux, D. Higher Mass-Independent Isotope Fractionation of
755 Methylmercury in the Pelagic Food Web of Lake Baikal (Russia). *Environ. Sci.*
756 *Technol.* **2012**, *46* (11), 5902–5911.

757 (74) Kritee, K.; Blum, J. D.; Johnson, M. W.; Bergquist, B. A.; Barkay, T. Mercury
758 stable isotope fractionation during reduction of Hg (II) to Hg (0) by mercury
759 resistant microorganisms. *Environ. Sci. Technol.* **2007**, *41* (6), 1889–1895.

760 (75) Perrot, V.; Epov, V. N.; Pastukhov, M. V; Grebenshchikova, V. I.; Zouiten, C.;
761 Sonke, J. E.; Husted, S.; Donard, O. F. X.; Amouroux, D. Tracing Sources and
762 Bioaccumulation of Mercury in Fish of Lake Baikal− Angara River Using Hg

763 Isotopic Composition. *Environ. Sci. Technol.* **2010**, *44* (21), 8030–8037.

764 (76) Kwon, S. Y.; Blum, J. D.; Carvan, M. J.; Basu, N.; Head, J. A.; Madenjian, C.
765 P.; David, S. R. Absence of Fractionation of Mercury Isotopes during Trophic
766 Transfer of Methylmercury to Freshwater Fish in Captivity. *Environ. Sci.*
767 *Technol.* **2012**, *46* (14), 7527–7534.

768 (77) Wang, R.; Feng, X.-B.; Wang, W.-X. In Vivo Mercury Methylation and
769 Demethylation in Freshwater Tilapia Quantified by Mercury Stable Isotopes.
770 *Environ. Sci. Technol.* **2013**, *47* (14), 7949–7957.

771 (78) Štrok, M.; Baya, P. A.; Hintelmann, H. The mercury isotope composition of
772 Arctic coastal seawater. *Comptes Rendus Geosci.* **2015**, *347* (7), 368–376.

773 (79) Mieiro, C.; Pacheco, M.; Pereira, M.; Duarte, A. Mercury Organotropism in
774 Feral European Seabass (*Dicentrarchus labrax*). *Arch. Environ. Contam.*
775 *Toxicol.* **2011**, *61* (1), 135–143.

776